Biosensors and Bioelectronics 126 (2019) 433–447

Contents lists available at ScienceDirect

Biosensors and Bioelectronics

journal homepage: www.elsevier.com/locate/bios

Advances in online methods for monitoring microbial growth

Xuzhi Zhang[a,b], Xiaoyu Jiang[a,c], Zhihui Hao[d,*], Keming Qu[a,b,**]

[a] Yellow Sea Fisheries Research Institute, Chinese Academy of Fishery Sciences, 106, Nanjing Rd, Shinan District, Qingdao 266071, China
[b] Laboratory for Marine Fisheries Science and Food Production Processes, Qingdao National Laboratory for Marine Science and Technology, Qingdao 266235, China
[c] College of Marine Sciences, Shanghai Ocean University, Shanghai 201306, China
[d] School of Chemistry and Pharmaceutical Sciences, Qingdao Agriculture University, 700, Changcheng Rd, Chengyang District, Qingdao 266109, China

ARTICLE INFO

Keywords:
Microbial growth
Online monitoring
Real-time
Sensor
Methodology

ABSTRACT

Understanding the characteristics of microbial growth is of great significance to many fields including in scientific research, the food industry, health care, and agriculture. Many methods have been established to characterize the process of microbial growth. Online and automated methods, in which sample transfer is avoided, are popular because they can facilitate the development of simple, safe, and effective growth monitoring. This review focuses on advances in online monitoring methods over the last decade (2008–2018). We specifically focus on optic- and electrochemistry-based techniques, either through contact measurements or contactless measurement. Strengths and weaknesses of each set of methods are described and we also speculate on forthcoming trends in the field.

1. Introduction

Research and application of microorganisms are currently flourishing in many fields, including in medicine, food industry, health care, agriculture, and environmental monitoring (Ahmed et al., 2014; Tonner et al., 2017). Characteristics of microbial growth, including their nutritional and energetic physiologies, and survival and proliferation under different conditions, are extremely valuable data to assess. Thus, understanding growth processes is of great significance for various goals related to the research and application of microorganisms (Schuler and Marison, 2012). For example, growth-based measurements are still considered the “gold standard” for antimicrobial susceptibility testing (Leonard et al., 2017; Theophel et al., 2014) and fermentation (Peris and Escuder-Gilabert, 2013). Numerous measurement methods have been established to assess the characteristics of microbial growth, and these are primarily based on descriptions of growth curves (Ahmed et al., 2014; Koch, 2007; Maia et al., 2016). According to the working model, they are generally divided into two categories: offline and online methods. Among offline methods, colony counting is still popular in some situations because it can provide conclusive and unambiguous results. However, it is a manual, operation-based method, is time-consuming, labor-intensive, and vulnerable to subjective errors, and also carries a high risk for contamination (Jung and Lee, 2016; Koch, 2007). Gene analysis-based methods, such as PCR and DNA sequencing, are also popular offline methods (Si et al., 2016; Syal et al., 2017; Zhang et al., 2017), and provide accurate results within a relatively short time (Gopinath et al., 2014). However, the tedious operations involved in gene-based analyses including manual sampling, primer design, DNA extraction and purification, among others, and their associated high costs decrease the likelihood of wide-scale application (Shao et al., 2016; Syal et al., 2017). Immunometric assays including enzyme-linked immunoabsorbent assays that use antigen-antibody reactions to detect individual microbial types are another commonly used offline method (Cho and Irudayaraj, 2013; Jain et al., 2012; Si et al., 2016; Wang et al., 2013). Though these assays provide sensitive and specific results, the analyses require considerable amounts of expensive reagents. The short shelf-life of such biosensors is another factor that limits the operational stability of these methods (Si et al., 2016). Lastly, sampling of culture medium or other solutions at discrete intervals to evaluate the growth of target microorganisms via measurements of optical density (OD) is another classical offline method (Lin et al., 2010). These techniques are generally time-consuming and cumbersome. In addition, the periodic manual sampling that is required and perturbation of incubation environments and growth can be problematic, especially for anaerobic microbes. Consequently, results from these methods cannot reflect accurate target information (Chai et al., 2008; Qiu et al., 2017; Sun et al., 2011). Therefore, increasing efforts have been recently geared towards online

* Corresponding author.
** Corresponding author at: Yellow Sea Fisheries Research Institute, Chinese Academy of Fishery Sciences, 106, Nanjing Rd, Shinan District, Qingdao 266071, China.
E-mail addresses: abplab@126.com (Z. Hao), qukm@ysfri.ac.cn (K. Qu).

https://doi.org/10.1016/j.bios.2018.10.035
Received 14 September 2018; Accepted 16 October 2018
Available online 18 October 2018
0956-5663/

methods.

In this mini-review, we summarize up-to-the-minute advances in online monitoring methods for microbial growth, discuss their emergence, and provide evidence-based opinions on the future aspects. We focus primarily on the most commonly used techniques. Given the vast number of publications in this area, we have primarily focused on those based on automated techniques and reports over the past decade. Even with this focus, we will unintentionally and inevitably exclude many exciting and emerging techniques in the growing body of literature. All of the figures in the paper are reprinted with permission from related publishers/authors, when it is necessary according to the journal's policy.

2. Methods based on optical techniques

In most cases, optic-based methods are non-invasive, non-destructive, contamination-risk free, do not interfere with the metabolism or culture microenvironments, and do not consume analytes. Therefore, they have the highest potential for adaptation into high-throughput formats. In this review, only methods without manual sampling steps are discussed. For the convenience of comparison, the features of each method are summarized in Table 1, and the details of typical protocols and applications for each method are briefly stated in the following sections.

2.1. OD

Using optical spectroscopies, OD measurements can be used to characterize the amount of scattered or absorbed light. OD values presumably correlate directly with microbial population sizes, thus providing an alternative to time-consuming hemocytometry and plate counting methods in order to monitor microbial growth (McBirney et al., 2017). OD measurement is one of the most important and viable methods that can be potentially adapted into a high-throughput format (Qiu et al., 2017). Moreover, they can easily be adjusted for special culture conditions (Toprak et al., 2012). Despite its popularity, the use of OD for directly studying microbial growth kinetics with traditional devices may yield problematic results (Lin et al., 2010). Therefore, considerable attention has been paid to its development.

Maia et al. (2016) introduced a strategy for turbidimetric monitoring of microbial growth in liquid cultures by employing an instrument consisting of a light source, a customized 3D printed culture tube holder, and a miniaturized spectrophotometer (the experimental setup and typical growth curves are shown in Fig. 1). The growth rates obtained with this simple method yielded no significant differences against those obtained using a benchtop spectrophotometer. And a high precision was observed.

Commercial systems for the online monitoring of microbial growth have been extensively studied. The use of forward laser light scatter (FLLS) to simultaneously measure the growth of multiple samples was evaluated by Hayden et al. (2016). Using these techniques, three isolates, *S. aureus*, *E. coli*, and *Pseudomonas aeruginosa,* were tested using the Vitek2 and MicroScan commercial antimicrobial testing systems. Comparisons indicated that the BacterioScan FLLS yielded a higher degree of categorical concordance. Further, Mao et al. (2017) presented a single path system for monitoring microbial growth using an open-source microprocessor board in shaker flasks that are commonly used in biological laboratories. A nonlinear calibration model of scattered light could then predict offline OD with a mean relative error of 5.2%.

Auxiliary devices including microfluidics-based systems have been developed for the continuous monitoring of microbial growth (Jakiela et al., 2013). For example, a system comprising approximately ten input and output channels controls more than 100 microdroplet chemostats and enables the independent manipulation of chemical factors in each microchemostat over time (Fig. 2). The dynamics of microbial populations in the microdroplet chemostats, and the cellular responses to a range of stable, or changing, antibiotic concentrations were characterized using a waveguide spectrophotometer that measured the absorbance of light. This method allowed for parallel, long-term studies of microbial ecology, physiology, evolution, and adaptation to chemical environments.

When microbial growth is monitored with optical methods, the scattering and absorbance of light from nanomaterials in the mixtures commonly act as interferences that complicate quantitative analysis. To address this issue, Qiu et al. (2017) developed an interesting solution by introducing large-scale dilution. The data analysis for this technique was inspired by that in quantitative PCR, where the delay in the amplification curve is correlated to the starting concentration of template nucleic acids. Fast and robust data analysis was achieved by developing computer algorithms. This high-throughput screening method would facilitate rapid screening of nanomaterial toxicity.

Some optic-based methods for monitoring microbial growth in real-time have also been developed by measuring metabolic products. Shao et al. (2016) demonstrated swift and accurate determination of CO_2 concentrations by use of a wavelength-modulated tunable diode-laser based absorption spectroscopy technique. The method produced high signal-to noise-ratio data, and both the maximum growth rate and lag time had a strong temperature dependence that matched conventional models for microbial growth very well. Using a dissolved oxygen sensor that was based on oxygen-sensitive organosilica microparticles, Kocincová et al. (2008) developed a phase-domain fluorescence lifetime-based method for simultaneously monitoring microbial growth in 24-well microplates. Further, Si et al. (2016) fabricated pH-sensitive fluorescent nanoparticles that did not influence microbial growth and were stable over several hours in a complex medium.

Measurement error in online monitoring of microbial growth would give rise to reproducibility problems in a wide range of applications. Therefore, it is critical that generated results are consistent. McBirney et al. (2017) compared the conventional OD_{600} methodology with a multi-wavelength normalized scattering optical spectroscopy method to measure the growth rates of *P. aeruginosa* and *S. aureus*. The results indicated that the multi-wavelength normalization process minimized the impact of metabolic products and environmental noise on the signal, thereby providing more accurate values with higher fidelity at low concentrations.

2.2. Imaging and microscopy

Fluorescent and chemically reactive molecular probes of cell envelope components allow the visualization of microbial growth, division, and antibiotic action, and advance our understanding of cell envelope biosynthesis. Hodges et al. (2018) synthesized a fluorogenic probe, i.e., a quencher-trehalose-fluorophore, enabling continuous live cell imaging in *Mycobacterium* and related genera. Then, they developed an online method for monitoring microbial growth with the help of a fluorescence microscope (Fig. 3). Similarly, Kuru et al. (2015) also developed an imaging method to monitor the growth of *E. coli* by using fluorescent d-amino acids that are the basis for illumination. Intriguingly, an in vivo fluorescent imaging method was also developed that could monitor the growth of *V. alginolyticus* polar flagella in real-time (Chen et al., 2017).

Chandra and Singh (2018) developed a unique system for monitoring microbial growth by using pH-sensitive carbon dots that determine pH changes resulting from metabolic activities. The system comprised a microgel that was constructed based on small scale culture platforms, in which a small concentration of microbial cells and nanoprobes were co-located. The changes in pH were immediately detected by carbon dots, allowing real-time measurements of cell activities at significantly lower concentrations than with fluorescence microscopy (Fig. 4).

London et al. (2010) presented a method for detecting and enumerating growing microcolonies over many generations using digital

Table 1
Online methods for monitoring microbial growth based on optical techniques.

Method	Properties							Reference
	Device	Identifying model	Auxiliary probe	Selectivity	Sampling	Temporal resolution	Channel	
OD	Miniaturized UV–Vis spectrophotometer	Direct density, automatic	No	No	*In situ*	1 h	Single	(Maia et al., 2016)
	BacterioScan system	Direct density, automatic	No	No	*In situ*	3 min	Multi	(Hayden et al., 2016)
	LED, photodiode	Direct density, automatic	No	No	*In situ*	5 s	Single	(Mao et al., 2017)
	Spectrophotometer, microdroplet chemostat	Direct density, automatic	No	No	Auto sampling	a few min	Multi	(Jakiela et al., 2013)
	UV–Vis spectroscopy	Direct density, automatic	No	No	Dilution	20 min	Multi	(Qiu et al., 2017)
	Diode laser, photo detector	Measure CO_2, automatic	No	No	*In situ*	No data	Single	(Shao et al., 2016)
	Dual optical sensor, SensorDish reader	Measure O_2, automatic	Organosilica microparticle	No	*In situ*	30 min	Multi	(Kocincová et al., 2008)
	UV–Vis spectroscopy	Monitor pH	Fluorescent organic nanoparticle	No	*In situ*	6 min	Multi	(Si et al., 2016)
	S1200 spectrophotometer	Multi-wavelength differential absorption spectroscopy	No	No	Dilution	15 min	Single	(Hodges et al., 2018)
Imaging	Fluorescence microscopy	Imaging fluorogenic probe in live cells	Quencher-trehalose-fluorophore	Yes	*In situ*	30 or ~5 min	Single	(Hodges et al., 2018; Kuru et al., 2015)
	Fluorescence microscope, LED, CMOS camera	Imaging cellular flagella	NanoOrange	Yes	*In vivo*	5 min	Single	(Chen et al., 2017)
	Fluorescence microscopy	Imaging fluorogenic carbon dot	Carbon dot	No	*In situ*	No data	Single	(Chandra and Singh, 2018)
	Analysis software, CCD, LED	Imaging cell autofluorescence	No	Yes	*In situ*	30 min	Single	(London et al., 2010)
	OCelloScope system	Time-lapse imaging 2D picture	No	Yes	*In situ*	1 or 20 min	Multi	(Fredborg et al., 2013; Wollenberg et al., 2016)
Microscopy	Inverted microscope, CCD camera	Monitor fluorescent protein	L-arabinose	Yes	*In situ*	15 min	Multi	(Sun et al., 2011)
	Microscopy, CMOS sensor	Bacterial microcolonies	No	Yes	*In situ*	20 min	Single	(Jung and Lee, 2016)
Diffraction	Microfluidic chip, diffraction optics	Diffractive intensity	No	No	*In situ*	15 min	Single	(Goh and Borisenko, 2017)
Refractive index	Tapered fiber, DFB laser, photodiode	Transmission change	Poly-L-lysine	No	*In situ*	12 min	Single	(Zibaii et al., 2010)
Raman scattering	Magnetic device, CCD detector, agitator	Intensity of Raman signal	SERS tag, antibody nanoparticle	Yes	*In situ*, Auto sampling	10–30 min	Multi	(Weidemaier et al., 2015)
Visualization	No	Color change with eye	Fluorescent nanoparticle	No	*In situ*	–	–	(Thakur et al., 2015; Wang et al., 2013)
	No	Color change with eye	Curcumin	No	*In situ*	–	–	(Kuswandi et al., 2012)

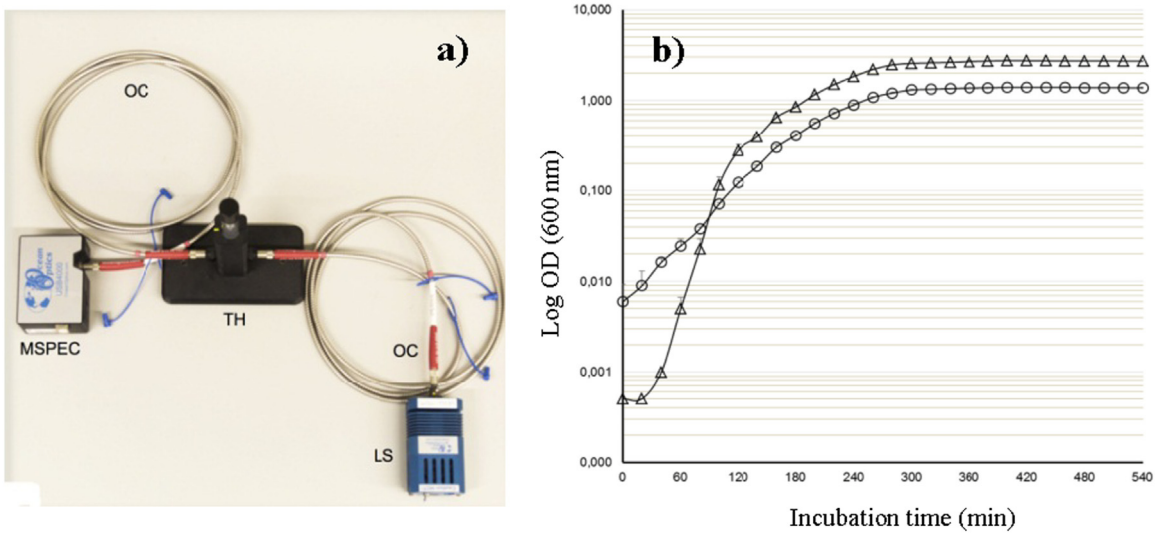

Fig. 1. The miniaturized setup used for monitoring microbial growth and obtaining typical growth curves. a) Detailed view of the tube holder. b) Growth curves of *E. coli* obtained by measuring the OD at 600 nm in the miniaturized setup (triangles), and the benchtop UV–Vis spectrophotometer (circles).

imaging of cellular autofluorescence. The method preserves the viability of the detected microcolonies, thus enabling generation of pure cultures for microbial identification. In comparison to visual colony counting that permits detection of *E. coli* colonies containing about 5×10^6 cells.

Commercial imaging systems (i.e., oCelloScope) for online monitoring have also been investigated in detail. Unlike other high-resolution imaging methods, oCelloScope does not capture the growth of individual cells, but rather a population of cells in liquids, and consequently eliminates the need to attach microbial cells to an inert surface. Fredborg et al. (2013) described an optical screening system of this type that is based on the time-lapse imaging of 96 bacterial-antibiotic combinations at a time (Fig. 5). The oCelloScope system provides fast high-throughput screening and a real-time method for detecting microbial antibiotic susceptibility by determining microbial growth kinetics as a result of image stack processing. The use of this system in studying the effect of a *Fusarium*-specific cyanoacrylate fungicide on the growth and morphology of four *Fusarium spp*. was reported by Wollenberg et al. (2016).

Jung and Lee (2016) reported an automated, real-time microbial microcolony-counting system that was implemented on a wide field-of-view, on-chip microscopy platform that was termed ePetri (Fig. 6). Using sub-pixel sweeping microscopy with a super-resolution algorithm, the system offered the ability to dynamically track individual microbial microcolonies over a wide field-of-view. Of note, its performance required neither stage nor lens moving. This approach not only provides results that are comparable to conventional colony-counting assays, but can also be used to monitor the dynamics of colony formation and growth, thereby representing a platform that could reduce the detection times of colony counting.

L-arabinose can induce recombinant microbes to synthesize green fluorescent protein, which can be used to assess temporal changes in

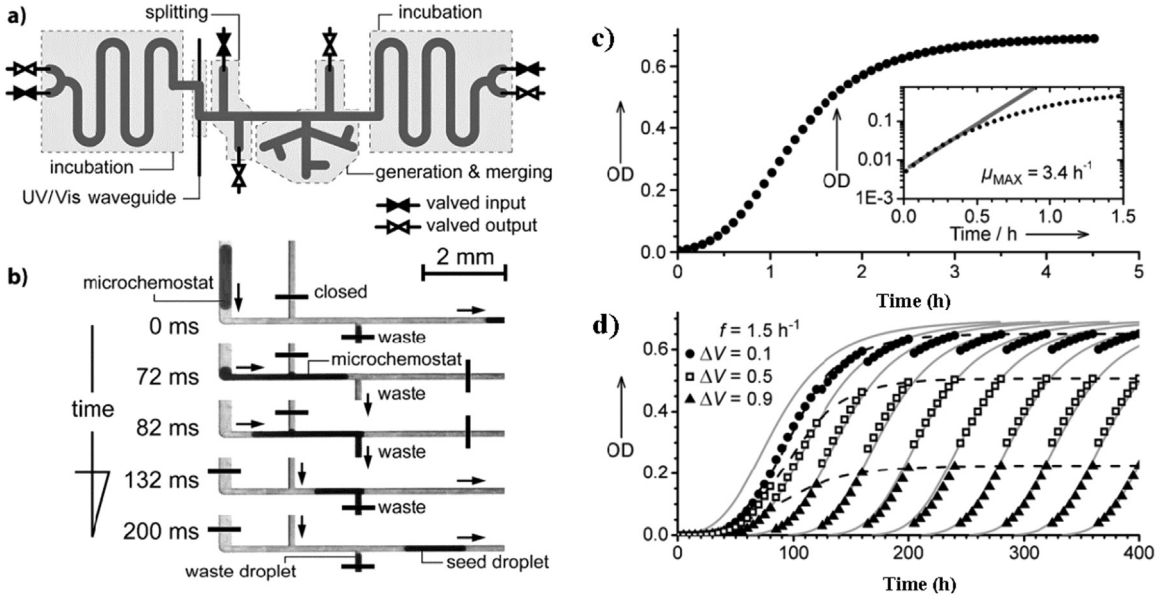

Fig. 2. a) Diagram of the microfluidic device layout. b) A sequence of micrographs illustrating the splitting of one microdroplet into a seed droplet and waste droplets with pre-programmed volumes. c) Representative growth curve of *E. coli* in a microdroplet chemostat. Inset: Calculation of the growth rate by fitting the exponential function. d) Three repetitive growth curves acquired over an extended period of time, and with different fractions of exchanged medium. Experimental data points were in good agreement with theoretical curves as depicted by Monod's model (gray lines).

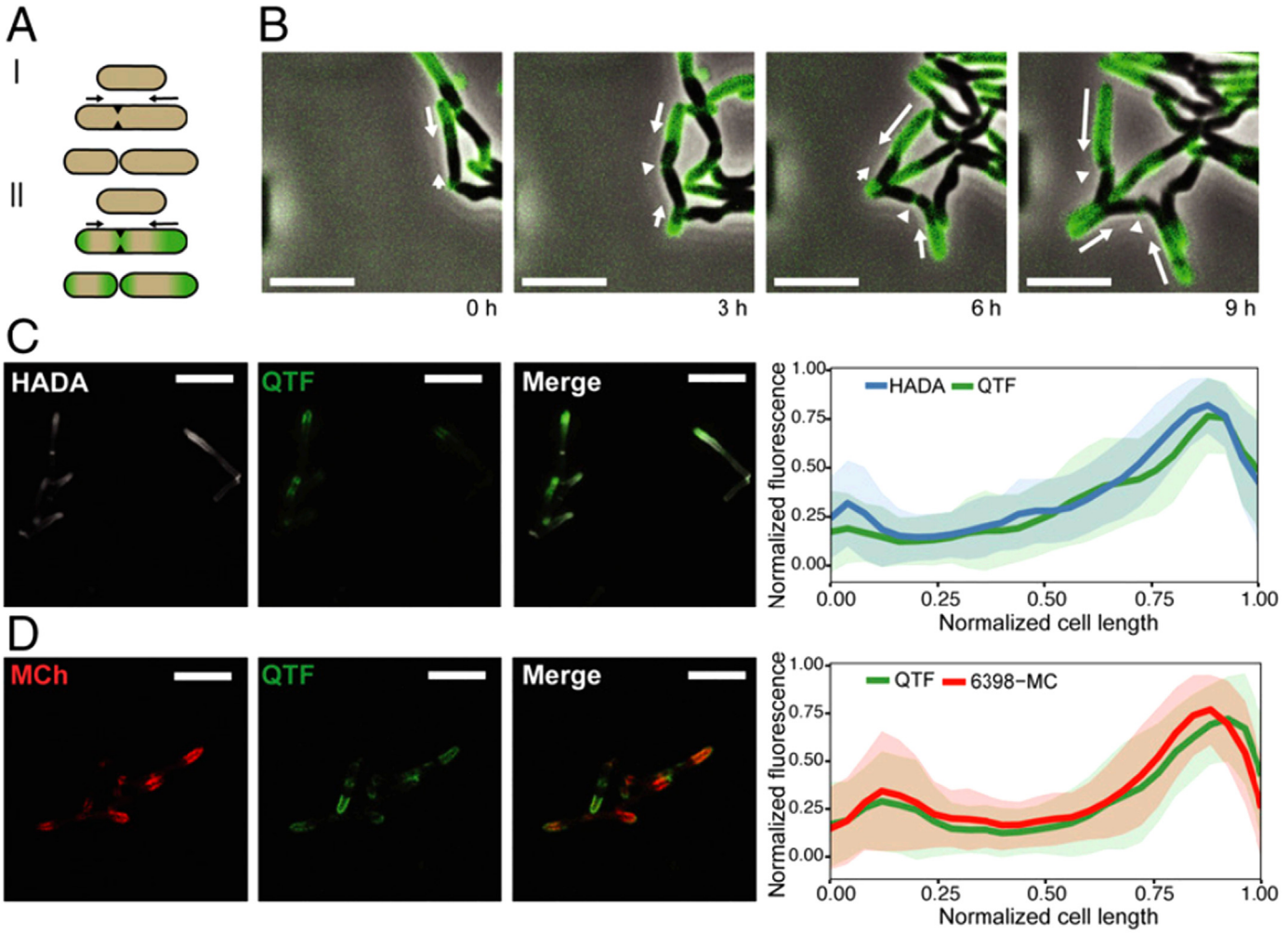

Fig. 3. Live-cell imaging of mycolyltransferase activity during growth and division of *M. smegmatis*. (A, I) Asymmetric growth model for Mycobacteria. (A, II) Summary of quencher-trehalose-fluorophore (QTF) fluorescence during *M. smegmatis* growth. (B) *M. smegmatis* was exposed to QTF (250 nM) and the cells were continuously monitored in a custom microfluidic device. White arrows depict the direction and magnitude of growth. Scale bar: 5 μm (C) 7-Hydroxycoumarin-3-carboxylic acid-3-amino-D-alanine (500 μM, pulse duration of 30 min, 10% of one doubling time) with 1 μM QTF. Scale bar: 5 μm. (D) *M. smegmatis* expressing an mCherry fused to mycolyltransferase Msmeg_6398 treated with QTF (1 μM). Scale bar: 5 μm. Error bars reflect standard deviations from all measured cells.

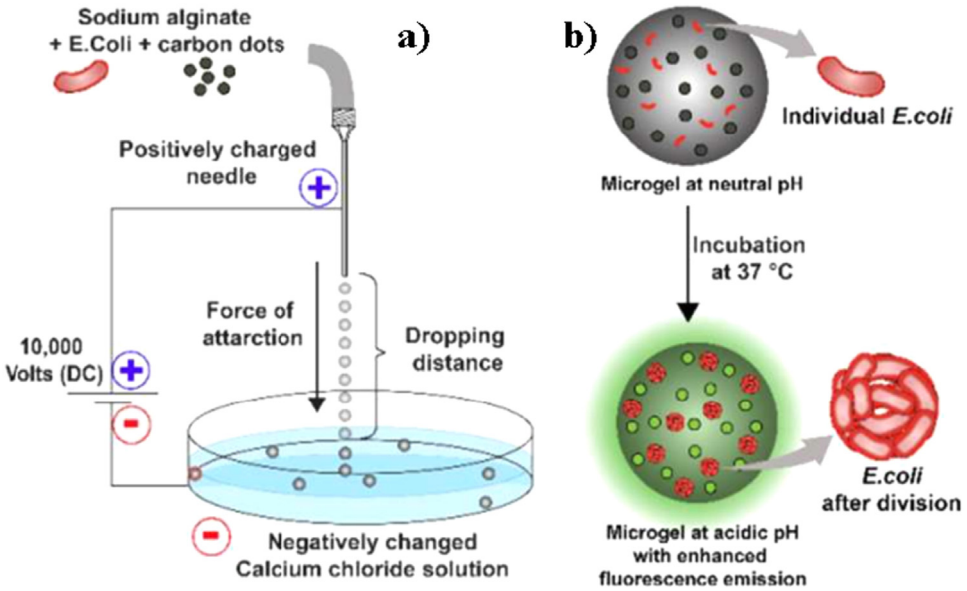

Fig. 4. a) Arrangement used for generating alginate microgels encapsulating *E. coli* and carbon dots. b) Cartoon showing growth of encapsulated *E. coli* resulting in enhancement of fluorescence emission due to decreases in pH.

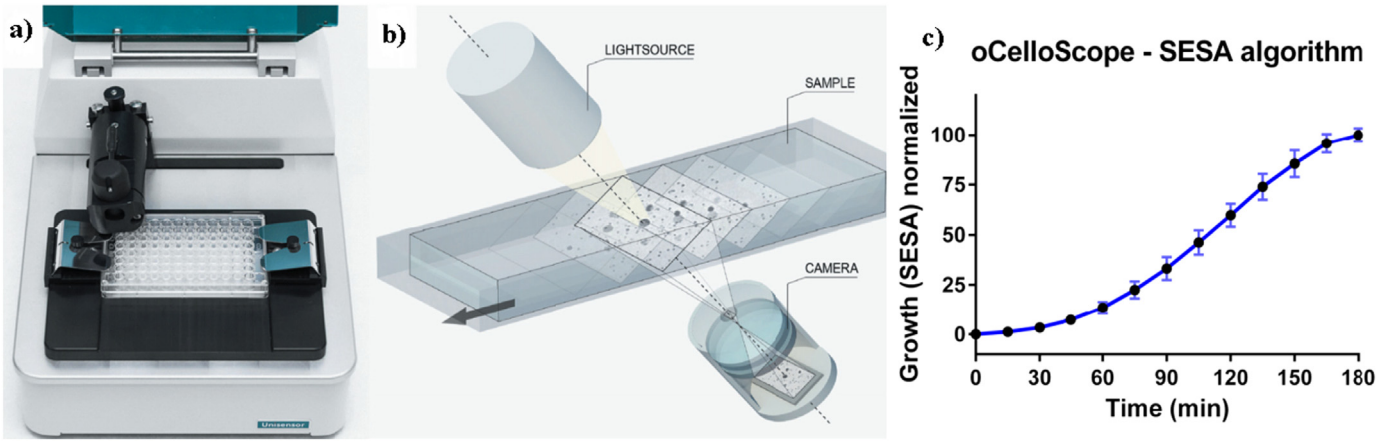

Fig. 5. a) Picture of the oCelloScope detection system with a standard 96-well plate inserted into it. b) Simplified engineering drawing of the detection principle. A 50 µL volume of a growing microbial culture is scanned, resulting in a stack of images. Each image can be transformed to a 2D picture. c) Growth is measured by oCelloScope segmentation and extraction of the surface area algorithm.

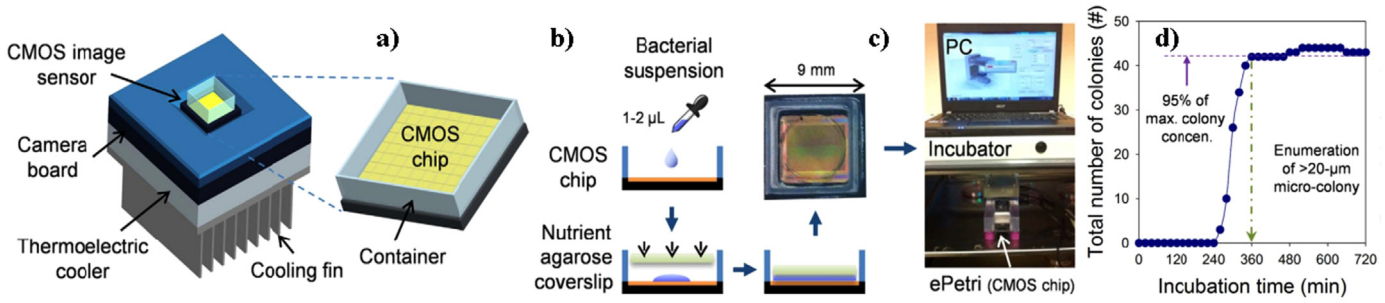

Fig. 6. Schematic diagram of the real-time microbial microcolony counter system using onchip microscopy. a) The ePetri platform consisting of a CMOS image sensor chip, a camera board, and a thermoelectric cooler with a cooling fin. b) The preparation procedure for real-time measurement of microcolonies consisting of only two steps: loading the microbial suspension onto the CMOS chip, and covering the CMOS chip with the nutrient agarose sheet. c) After the preparation steps, the ePetri platform is placed inside an incubator to commence the acquisition of time-series images of microcolonies. d) An example growth curve obtained from the system using on-chip microscopy.

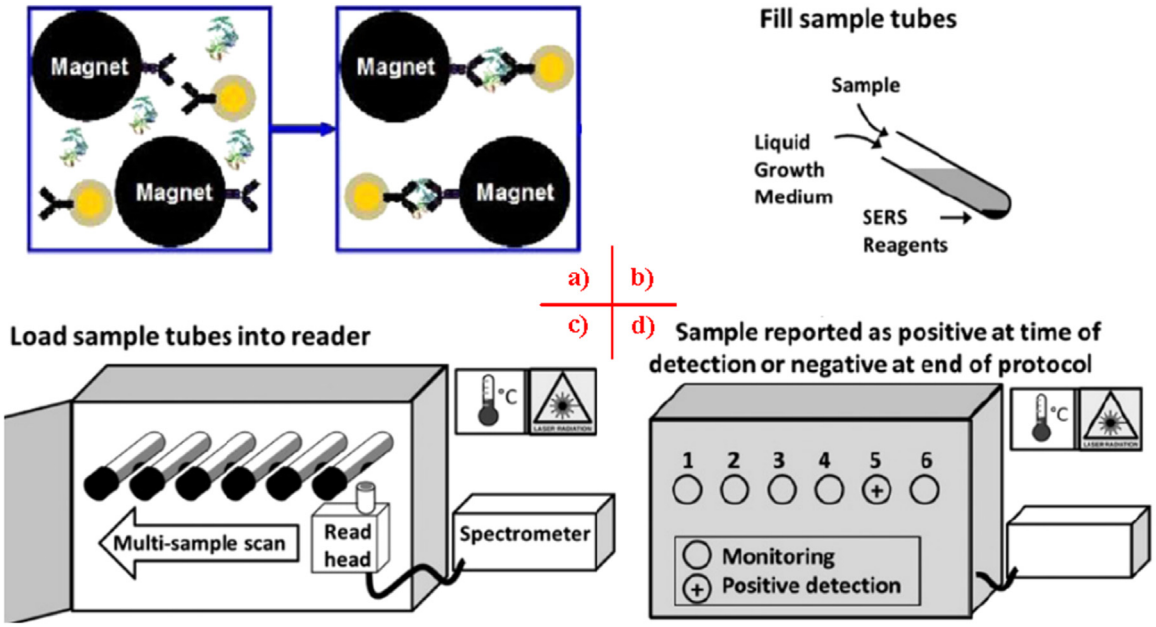

Fig. 7. a) Representation of the SERS assay format, in which the target pathogen is “sandwiched” between SERS tags and superparamagnetic microparticles that are conjugated with antibodies specific for the pathogen. b) Standard culture tubes with screw caps are loaded with the sample, growth medium, and SERS nanoparticles. c) The culture tubes are then loaded into the SERS reader, and incubation of the samples at controlled temperatures results in the formation of pellets in the samples on a predetermined schedule, and the pellets are scanned by Raman readings across the pellets. d) Samples are reported to the user as positive or negative when growth is detected.

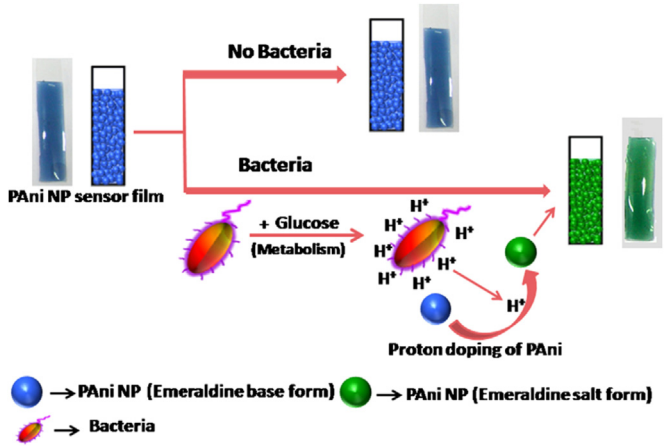

Fig. 8. Schematic representation of the mechanism for monitoring microbial growth using a polyaniline nanoparticle- based colorimetric sensor.

fluorescent signals via microscopy and imaging analysis. Determination of the temporal changes in total fluorescence intensity of the area occupied by fluorescent substances allows to monitor various stages of growth in real-time. Based on this, Sun et al. (2011) developed a high-throughput microfluidic system for the long-term culture and monitoring of *E. coli* HB101.

2.3. Diffraction

Light diffraction is a straightforward, effective, and low cost analytical tool for monitoring kinetics and is used in quantification applications. Goh and Borisenko (2017) reported a diffraction-based sensor incorporated into a microfluidic chip that captures microbial cells in an array of traps and permits the monitoring of their growth rates in a controlled environment. The diffraction method provides statistically relevant data by averaging over a large number of diffraction centers that then enables data collection and quantification without cell labelling, staining, or tracking. Therefore, the system is particularly suitable for real-time monitoring of ongoing processes in microbiological systems and could be extended to monitoring individual cells within communities comprising different microbial species.

2.4. Refractive index

By employing lasers and photodiodes, Zibaii et al. (2010) developed an online method for monitoring microbial population growth. *E. coli* were immobilized on the internal surface of a special taper. During their growth, the refractive index of the tapered region increases, resulting in changes of optical throughput.

2.5. Raman spectroscopy

Based on the employment of Surface Enhanced Raman Scattering (SERS) and homogeneous immunoassays, Weidemaier et al. (2015) reported an approach for the real-time detection and identification of pathogens in complex culture matrices (Fig. 7). SERS-labeled immunoassay nanoparticles are included in the cultural enrichment vessel, and the signal is monitored in real-time through the wall of the vessel, while cultivation is ongoing. The continuous monitoring of specific populations loaded throughout the enrichment process enables rapid hands-free detection without interfering with microbial growth, and significantly reducing the risk of contaminating the culture. However, there are limitations of unsatisfactory stability and robustness.

Table 2
Online methods for monitoring microbial growth based on electrochemical techniques.

Pattern	Properties							Reference
	Device	Identifying model	Auxiliary probe	Selectivity	Sampling	Temporal resolution	Channel	
Impedance	Impedance analyzer, gold electrode, agitator	Contact impedance	No, label free	No	No	1 h	Single	(Kim et al., 2009; Varshney and Li, 2009)
	Impedance analyzer, micro-gold electrode	Contact impedance	No, label free	No	No	1 h	Single	(Settu et al., 2015)
	xCELLigence Real-Time Cell Analyzer	Cell index value of biofilm	No, label free	No	No	15 min	Multi	(Duuren et al., 2017; Ferrer et al., 2017)
	Impedance analyzer, gold electrode	Impedance of solid medium	No, label free	No	No	2 h	Single	(Choi et al., 2009)
Capacitance	Capacitive sensor, microfluidic chip	Capacitance of biofilm	No, label free	No	No	7.5 min	Single	(Ghafar-Zadeh et al., 2010)
	Capacitance sensor, capacitance analyzer	Contact capacitance	Aptamer	Yes	No	~3 min	Multi	(Jo et al., 2018)
Contact conductivity	CMOS conductometric IC, electrodes	Resistance change	No, label free	No	No	Continuous no clear data	Multi	(Yao et al., 2011)
	CH-Instruments, electrodes	Resistance change	Nafion	No	No	Continuous no clear data	Single	(Chinnathambi and Euverink, 2018)
Magnetic field telemetry	Remote-query magnetoelastic sensor	Frequency of adhesion	No, label free	No	No	1 min	Single	(He et al., 2009; Huang et al., 2008, 2010)
Field effect	Field effect transistor, operating circuit	Voltage	No, label free	No	No	Continuous no clear data	Single	(Matsuura et al., 2013)
	Field effect transistor, Keithley source meter	Current result from pH change	No, label free	No	No	Continuous no clear data	Multi	(Ibarlucea et al., 2017)
Contactless conductivity	Contactless conductivity detector	Noninvasive, C^4D value	No, label free	No	No	Sub-second	Multi	(Zhang et al., 2018)

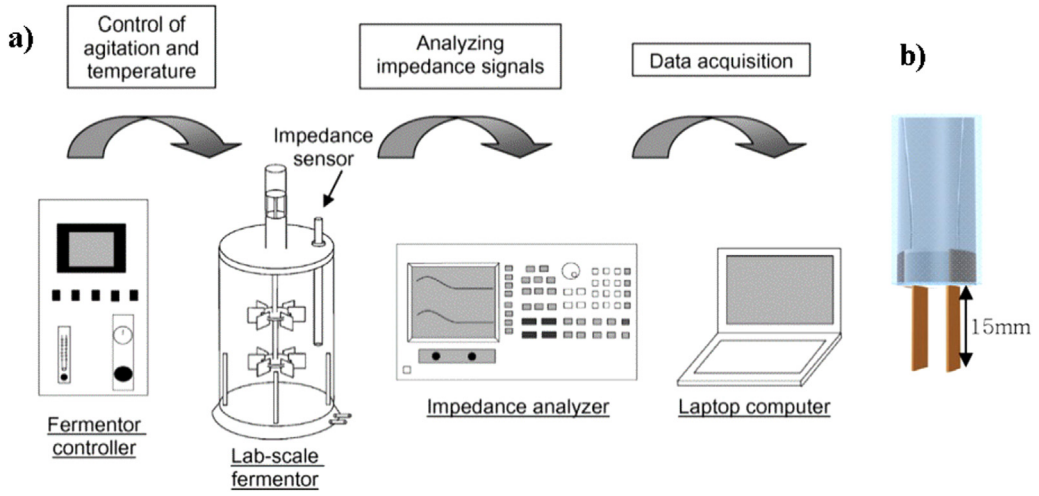

Fig. 9. a) Experimental setup of in situ monitoring of microbial growth with an impedance sensor. b) Schematic diagram of the working impedance electrodes.

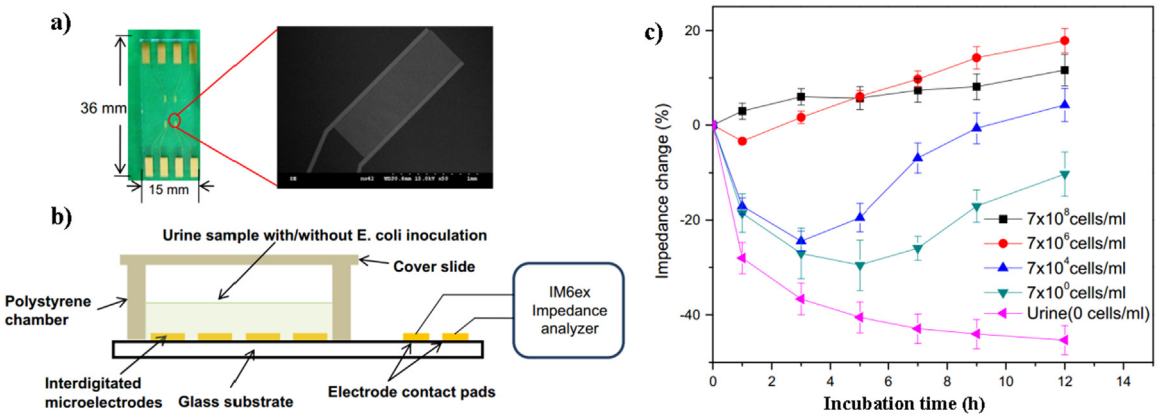

Fig. 10. a) Photograph of an interdigitated microelectrode sensor. b) Cross-sectional view of the interdigitated microelectrode sensor, polystyrene chamber, and urine sample during impedance measurement. c) Impedance change over time at 10 Hz within the first 12 h of cultivation, where initial *E. coli* cell abundances ranged from $7 \times 10^{\circ}$ to 7×10^{8} cells/mL.

2.6. Visualization

Solution phase colorimetric methods that utilize chromogenic or fluorescent probes carries constraints due to turbidity that is encountered during microbial growth. Nevertheless these methods have become very important tools for the investigation of microbial viability. Colorimetric methods, including visualization-based patterns, are more sensitive than plate counting and provide quicker results, even with turbidity of the complex matrix (Jung et al., 2017). In addition, it is advantageous to use sensor films that show a visual color change that can be observed macroscopically during the decomposition of food or after pathogen growth. Thakur et al. (2015) reported a simple colorimetric sensor for detecting microbial growth that relies on estimating the presence of metabolic products. pH-sensitive polyaniline nanoparticles are added to an agarose gel to fabricate a sensing film (Fig. 8). It has great potential for adaptation in real world applications in the form of patch sensors on cartons to gauge the integrity and freshness of food items and beverages in real-time. Similarly, other two colorimetric methods, developed by Wang et al. (2013) and Kuswandi et al. (2012), also work by the triggering of interactions between sensor particles and metabolic products released by microbial metabolisms.

3. Methods based on electrochemical techniques

Electrochemical methods have numerous well-known characteristics including relatively simple instrumentation, easy miniaturization, cost-effectiveness, and easy automation of measurements (Ahmed et al., 2014; Drummond et al., 2003; Peris and Escuder-Gilabert, 2013), making them attractive tools for monitoring microbial growth. Direct and indirect measurements are commonly based on sensing changes in electrical properties of medium or electrode surfaces. The required time for detectable changes depends on inoculum size, and if conditions are permissible for growth. Insufficient selectivity and reproducibility in real applications of these methods have been key problems limiting their popularization (Peris and Escuder-Gilabert, 2013). To address these issues, many advances have been reported recently. The main characteristics of these methods are summarized in Table 2, and the details of some typical methods are briefly described in the following sections.

3.1. Impedance and capacitance sensors

Impedance and capacitance spectroscopy are sensitive techniques to characterize the chemical and physical properties of solid, liquid, and gas phase materials. Microbial growth increases the conductivity of medium by converting uncharged, or weakly charged, substances in the growth medium (e.g., yeast, peptone, and sugar) into highly charged substances like amino acids, aldehydes, ketones, acids, and other metabolic products (Varshney and Li, 2008, 2009; Wawerla et al., 1999). In some instances, the new cells can attach to the surface of working electrodes, resulting in changes of impedance and capacitance. The attractiveness of impedance and capacitance methods is due to the

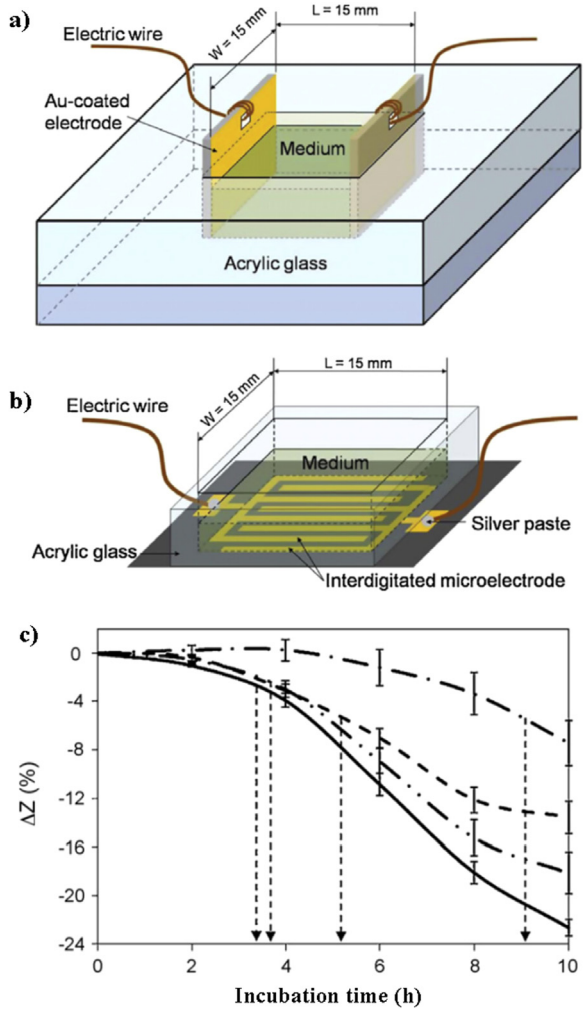

Fig. 11. Illustration of solid medium impedance sensors and typical growth curves. The solid medium sensor is filled with solid medium. a) Two gold-coated silicon electrodes are placed at adjacent sides of the well. b) Interdigitated microelectrodes are placed at the bottom of the well. c) Detection time for the solid medium sensor according to varying initial bacterial numbers. *B. subtilis* growth on the solid medium surface at 10^2 (–·–), 10^3 (– – –), 10^4 (–··), and 10^5 (—) initial cell numbers. The arrows represent the detection time.

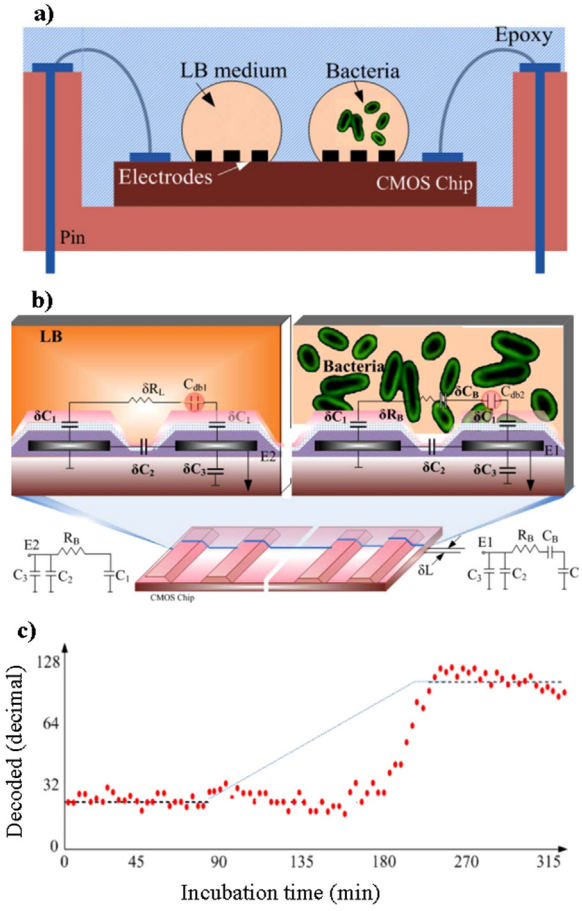

Fig. 12. a) Illustration of the fully differential microbial growth monitoring system using an on-chip capacitance sensor. b) Electrical model of the LB medium and microbial solution. c) Measurements of the decoded output over time for 10^7 CFU/mL *E. coli* in LB medium.

beneficial feature of measuring microbial metabolites and other related kinetics, in addition to the ability to discriminate between live and dead bacterial cells. Additionally, electrode surfaces can be reused in several different tests if there is no bio-recognition element that is used on the surface of working electrodes (Varshney and Li, 2009).

The total impedance resulting from microbial growth actually consists of two components: the medium or electrolyte impedance and the electrode/electrolyte interface impedance, and the two impedances can be measured in different frequency ranges. Kim et al. (2009) described an in situ impedance sensor for estimating microbial concentrations in a lab-scale fermentor. The experimental set-up and disposable working electrodes are shown in Fig. 9. As growth of *E. coli* increased, impedance increased, and reactance decreased over the experimental period. The correlation between *E. coli* population sizes and the impedance data was linear, although there was considerable fluctuation of impedance signals. However, multiple uses of working electrodes are not recommended because the surfaces require cleaning prior to reuse due to the adherence of cells and other biological materials to the electrodes.

Settu et al. (2015) developed an interdigitated gold microelectrode-based impedance sensor to detect *E. coli* by monitoring microbial growth (Fig. 10). An equivalent electrical circuit model was used to evaluate variation in impedance characteristics associated with growth. Analysis of the equivalent circuit indicated that changes in impedance values at low frequencies were caused by double layer capacitance resulting from microbial attachment and the formation of biofilms on the surface of the working electrode. A linear relationship was obtained between the impedance change and initial *E. coli* cell numbers.

New methods have been recently developed based on the commercial impedimetric analyzer, including the xCELLigence Real-Time Cell Analyzer MP. Ferrer et al. (2017) assessed the effects of antibiotics on microbial biofilm growth in real-time by measuring impedance in 96 × microtitre plates with gold electrodes at 15 min time intervals over 24 h. The impedance data appeared to reflect both microbial growth and matrix production, thus representing a measurement of total biofilm mass production. Further, Duuren et al. (2017) described the use of single frequency impedance spectroscopy to characterize the growth dynamics of *P. aeruginosa* biofilms in a label-free manner over a period of 72 h.

Choi et al. (2009) fabricated an impedance sensor by integrating solid medium and two plane electrodes that were attached on adjacent sides of an acryl well (Fig. 11). During analysis of impedance, the solid medium displayed characteristics consistent with a homogenous conductive material. Impedance changes of the solid medium were measured every 2 h during microbial growth over 10 h. Results indicated that lower conductivity medium were optimal for monitoring microbial growth due to the low threshold in variance of the impedance signal.

Ghafar-Zadeh et al. (2010) developed a complementary metal–oxide semiconductor capacitance sensor for the online monitoring of

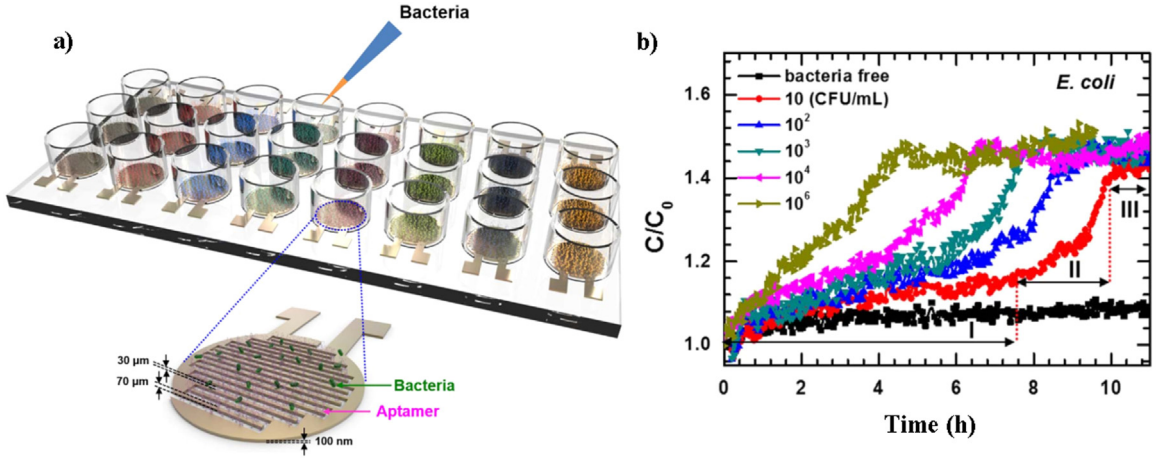

Fig. 13. a) Schematic of an aptamer-functionalized capacitance sensor array. DNA aptamers are immobilized onto the sensor surface between electrodes and microbes that are recognized by aptamers contribute to increasing capacitance. b) Curves of capacitance against incubation times with cultivation of different abundances of *E. coli.*

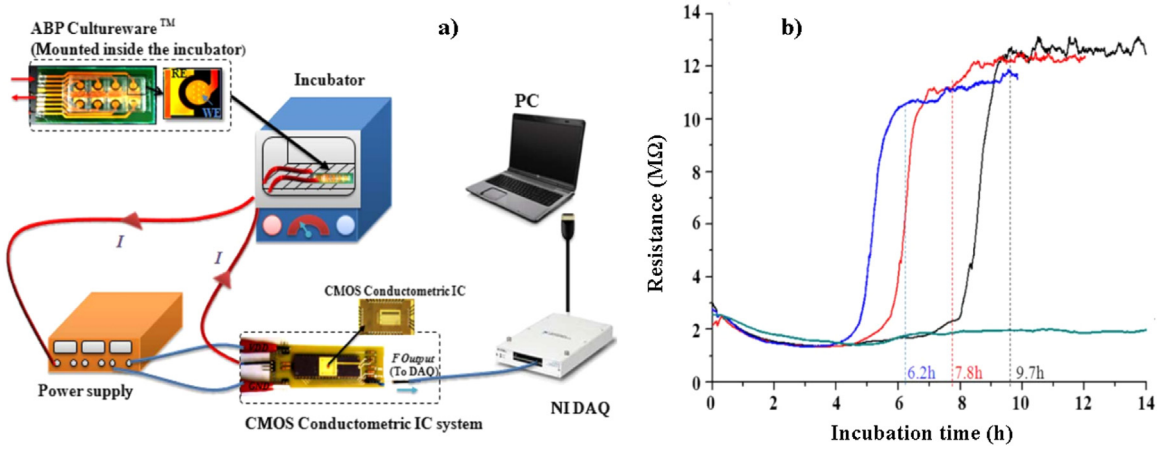

Fig. 14. a) Experimental setup for the microbial growth monitoring system based on contact conductivity measurements. b) Measured resistance characteristic curves to monitor the growth of *E. coli* at different initial cell numbers.

microbial growth. The sensor featured a differential capacitance readout architecture with both reference and sensing interdigitized electrodes, which were exposed to pure LB medium and *E. coli* suspended in LB medium, respectively. The illustration, electrical model, and capacitance of the sensing electrode over time are shown in Fig. 12. The proposed sensor represented the basic requirements for monitoring microbial growth, but further modifications would be necessary over the structure of the system in order to optimize it.

Jo et al. (2018) reported a method for monitoring microbial growth in real-time, termed the aptamer-functionalized capacitance sensor array. A schematic of the system and a typical growth curve produced by it are shown in Fig. 13a and b, respectively. The number of live cells bound to the sensor surface via aptamers is closely related to the capacitance. Thus, microbial growth can be monitored in real-time by measuring changes in capacitance. Growth of target microbes could be identified within 1 h due to the selectivity of the aptamers, although responses fluctuated considerably.

3.2. Contact conductivity

The metabolic activity of live microbes generally increases the ionic strength of medium, thereby increasing conductivity. Thus, methods based on measuring conductivity have been widely used for automatically monitoring microbial growth (Yang et al., 2005). However, if the microbes attach to the surface of the working electrodes, the resistance of the whole measurement circuit will increase because the resistance coefficient of a cellular membrane is much more insulating than the culture medium (Yang and Bashir, 2008). Based on this principle, Yao et al. (2011) developed a method for online monitoring microbial growth using a complementary metal–oxide semiconductor (CMOS) conductometric integrated circuit. The experimental setup of the system and typical growth curves obtained are shown in Fig. 14. A unique property of the system is that an extremely low initial concentration of cells could be monitored, which is difficult to achieve with many large sized commercially available systems.

Using voltammetric and conductometric methods to monitor microbial growth in a common culture medium or in a complex fermentation medium brings several challenges. In particular, metabolic activities produce chemically active products and electrochemically active redox species that can interfere with sensor performance. Chinnathambi and Euverink (2018) developed a simple approach to effectively avoid this interference by coating Nafion films over the working electrode. Using a polyaniline functionalized, electrochemically-reduced graphene oxide working electrode, continuous monitoring of the *Lactococcus lactis* fermentation process was performed by recording the change in resistance of the fermentation medium.

3.3. Magnetic field telemetry

Though methods based on electrochemical techniques exhibit

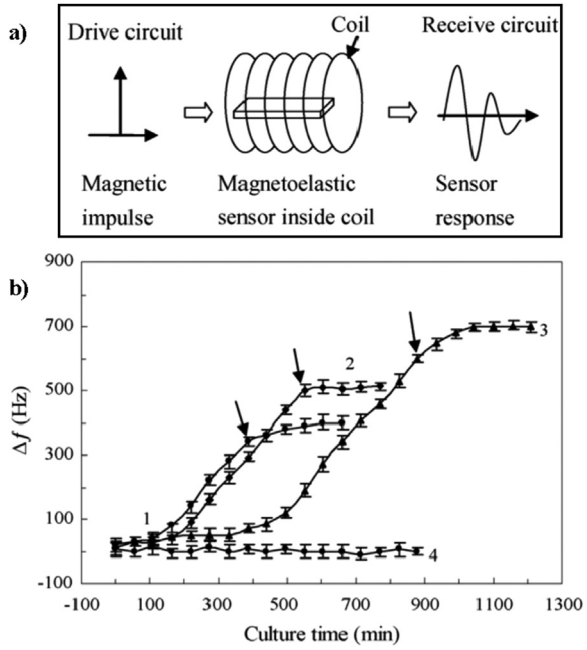

Fig. 15. a) Operation of the wireless magnetoelastic sensor. b) The time dependent shift in magnetoelastic sensor resonance frequencies, and CM 2–1 medium, as a function of initial *E. coli* cell abundances: 1—3 × 10^6 CFU/mL; 2—3 × 10^4 CFU/mL; 3—2 × 10^2 CFU/mL; 4—Negative control.

several advantages, electrode deterioration and nonspecific binding are unavoidable since working electrodes must be in galvanic contact with the medium. The requirement of a reference electrode is invasive and possibly causes increases in potassium chloride impurities that may have a big impact on medium. These issues result in erratic measurements that then decrease the accuracy of the methods (Chinnathambi and Euverink, 2018; Ong et al., 2001). Consequently, commercial success of these methods has been rare, due primarily, to variable reproducibility (Ahmed et al., 2014). To address this challenge, breakthroughs have been made by employing a wireless, remote, query resonant-circuit sensor. The resonance frequency of a liquid-immersed magnetoelastic sensor measured through magnetic field telemetry generally changes in response to microbial adhesion to the sensor and the liquid properties of the medium (e.g., viscosity, density, elasticity). Subsequently, the decrease allows the enumeration of microbial cells. The lack of any physical connection between the measurement sensor and the culture medium facilitates aseptic operation and avoids electrode deterioration, making the platform ideally suited for online monitoring. Huang et al. (2008) developed a method for detecting the growth of *E. coli* O157:H7 in real-time using this type of sensor (Fig. 15). Shortly thereafter, the same research group reported its use in the quantification of *S. epidermidis* (Huang et al., 2010). In addition, He et al. (2009) reported a similar method for online monitoring of *Mycoplasma genitalium* growth.

3.4. Field effect

The field-effect transistor involves a single-carrier-type operation, and is also known as a unipolar transistor. The system uses an electric field to control the electrical behavior of the device. In pH-sensitive field-effect transistors, the electrical signal that is generated depends on the surface potential of a gate insulator that can be modified by the accumulation of charges at the insulator surface. These charges are resultant from changes in pH within the solution (Lee et al., 2009). Matsuura et al. (2013) reported a method for measuring microbial growth in suspensions that is based on an ion-sensitive field-effect transistor. Further, biofilm formation was measured in microfluidic channels. Ibarlucea et al. (2017) reported a method capable of detecting microbial growth by employing a nanoscale honeycomb-patterned silicon nanowire field effect transistor (Fig. 16). The use of such a field-effect transistor enabled the quantification of parameters that were not easily accessible by conventional optical methods in a label-free manner.

3.5. Contactless conductivity

Many of the complex components in culture medium have a tendency to influence the properties of electrochemical electrodes, resulting in lessened accuracy and reproducibility of measurements. To eliminate this interference, commonly additional steps, such as renewal, are necessary. These requirements impair the ability of contact electrochemical methods to online monitor microbial growth with high resolution. Moreover, the invasive nature of the process may introduce the risk of contamination, or disturb the incubation conditions (Syal et al., 2017). To address this issue, Zhang et al. (2018) developed a system for noninvasive online monitoring of microbial growth by employing a multichannel capacitively-coupled contactless conductivity detector (C^4D) as a sensing component to record changes in conductivity of medium. The working principle, structure, picture of the head stage, and typical growth curves obtained are shown in Fig. 17. Unlike some common methods, it doesn't require any chemical (e.g., pH-sensitive fluorescent nanoparticles (Si et al., 2016)), biotic (e.g., antibodies (Goh and Borisenko, 2017) and aptamers (Jo et al., 2018)) or physical (e.g., magnetic beads (Kinnunen et al., 2011)) compounds as indicators or auxiliary materials.

4. Methods based on the magnetic bead rotation microviscometer

Single microbial cell growth can be directly and continuously observed using optical imaging methods (Chandra and Singh, 2018; Chen et al., 2017; Deris et al., 2013; Hodges et al., 2018; Kuru et al., 2015). However, there are limitations to using these methods based on issues inherent to diffraction and interference in absorption. Kinnunen et al. (2011) reported a high-resolution method to address the problem by employing an asynchronous magnetic bead rotation sensor (Fig. 18). A

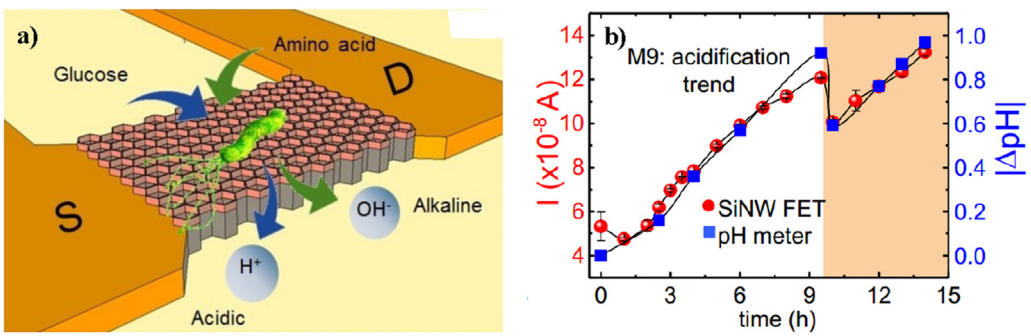

Fig. 16. a) Conceptual schematic of the field effect transistor measurement. The effects of microbial activity are measured on a field effect transistor consisting of a silicon nanoweb and electrodes. b) pH change in the absolute value and field effect transistor signal during microbial incubation in medium, including the addition of 30% fresh medium after saturation was observed.

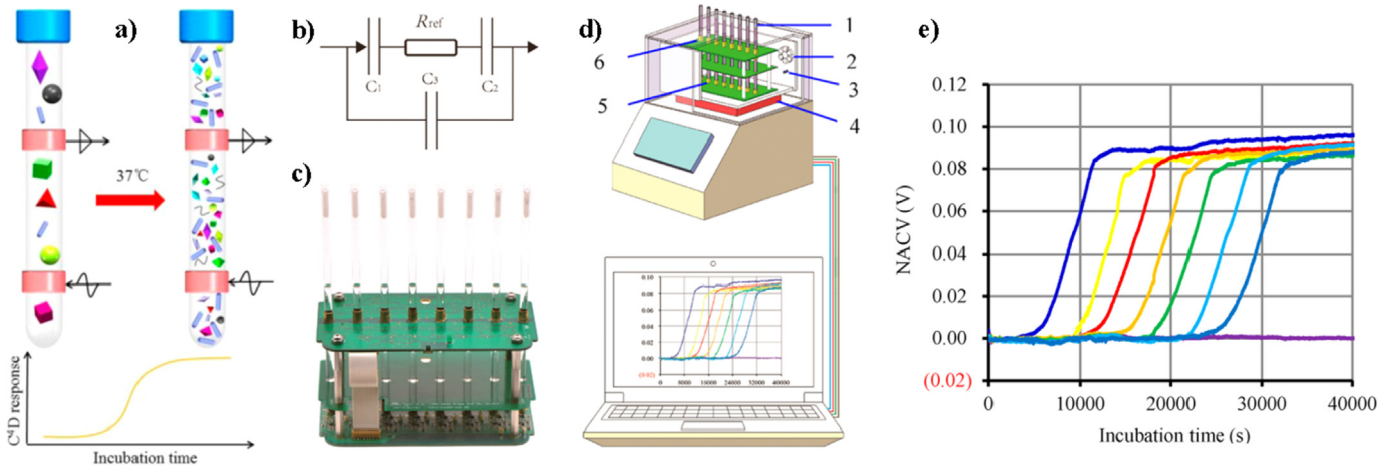

Fig. 17. Online monitoring of microbial growth with the multichannel C^{4}D. a) Illustration of the working principle. Microbial growth activity transforms uncharged or weakly charged substrates into highly charged end products, increasing the conductivity of the medium. b) The practical equivalent circuit of each unit of C^{4}D. c) Photograph of the head stage of the eight-channel C^{4}D, with eight culture tubes inserted. d) Schematic of the device, consisting of two key functional modules (i.e. temperature control and conductivity data collection). 1—bacterial culture tube; 2—mini electronic fan; 3—temperature sensor; 4—thermoelectric cooler; 5—actuator electrode; and 6—pick-up electrode. e) Typical growth curves from different initial *E. coli* abundances in LB medium. From left to right, the initial inocula of *E. coli* were 1.54×10^9, 1.54×10^8, 1.54×10^7, 1.54×10^6, 1.54×10^5, 1.54×10^4, and 1.54×10^3 CFU, respectively.

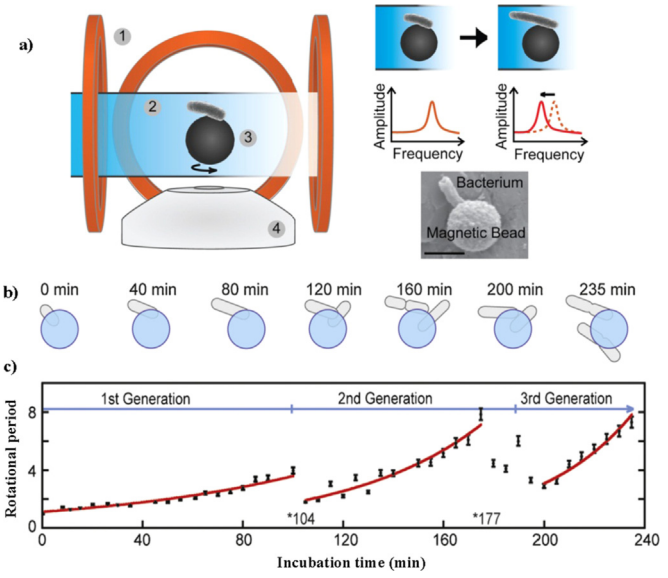

Fig. 18. a) Conceptual diagram for measuring single microbial cell elongation using the asynchronous magnetic bead rotation method. An asynchronous magnetic bead rotation sensor is placed on a microscope. 1-electromagnet coils, 2-the fluidic sample, 3-the asynchronous magnetic bead rotation sensor with an *E. coli* cell attached, 4-the microscope objective. The elongation of the attached cell increases the system's effective volume, causing a change (indicated as a peak shift) in the rotational period of the sensor-bacterium complex. The single *E. coli* cell is attached to a 2.8 μm magnetic bead as shown by the scanning electron microscopy image. b) Schematic figures of the asynchronous magnetic bead rotation sensor with an initial single cell attached, followed by subsequent cell divisions. c) Cell growth and division as observed with the asynchronous magnetic bead rotation sensor. After a period of growth, the first cell division was observed at 104 min and again at 177 and 199 min. The error bars correspond to the measurement error in the rotational period and the exponential fits were used to aid interpretation.

single *E. coli* cell was immobilized onto the surface of a magnetic bead via immune capture. The growth of the cell was then online monitored by varying the torque-based magnetic bead sensor over multiple generations. In another study (Sinn et al., 2012), the same research group reported that the minimum inhibitory concentration of gentamicin for *E. coli* could be obtained within 100 min using this method.

5. Methods based on microcalorimetry

Microbial growth involves metabolic processes that generate heat. The heat flow rate is proportional to reaction rates, and the total heat produced over some time period is proportional to the extent of the reaction that takes place in that period. This principle makes isothermal microcalorimetry a useful, non-specific tool for evaluating microbial growth with the integration of proper mathematical models. Bonkat et al. (2012) reported a method for online monitoring of microbial growth based on isothermal microcalorimetry that could provide continuous data with high resolution. The experimental setup and typical heat flow curves are shown in Fig. 19. The authors demonstrated that the innovative method was useful in investigating the growth of urinary pathogens in sterilized urine. von Ah et al. (2009) also demonstrated the feasibility of monitoring the growth of *E. coli* and *S. aureus* with an isothermal microcalorimetry instrument by continuously recording changes in heat.

6. Methods based on resonant mass

Cantilevers containing small channels that facilitate microbial passage can be made to vibrate continuously. When microbes pass through the channel, the change in weight results in a change in the frequency of cantilever movement. The principle of monitoring microbial growth based on resonant mass has been demonstrated, and some preliminary trials of feasibility have been published (Knudsen et al., 2009). Godin et al. (2010) reported a dynamic fluidic control system that enabled the online measurement of non-adherent microbial cell buoyant mass with a suspended microchannel resonator (Fig. 20). In addition, Cermak et al. (2016) presented a high-throughput approach based on a resonant mass sensor to precisely and rapidly measure microbial growth of many individual cells simultaneously.

7. Methods based on gene analysis

As stated above, it is difficult to use gene analysis for online monitoring of microbial growth due to sampling requirements and other complicated operations that are time-consuming. However, there have been recent developments in methods of gene-based applications. Zhang et al. (2017) reported the development of a method for evaluating the characteristics of growth for three phylogenetically distant anammox microbial species by directly measuring 16 S rRNA gene copy

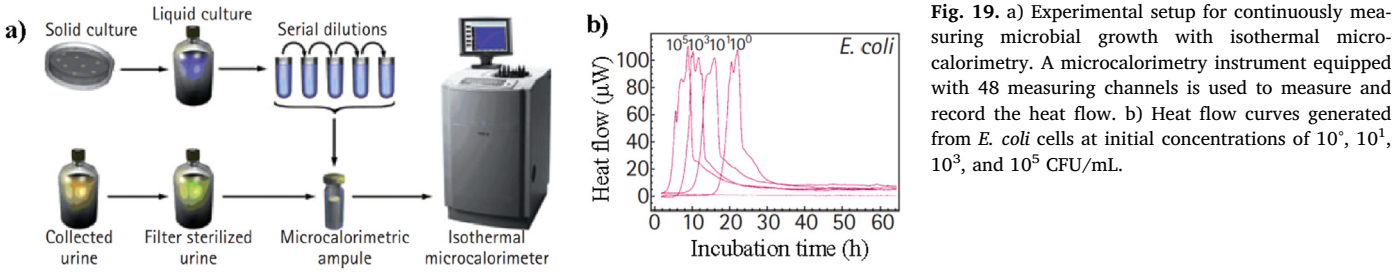

Fig. 19. a) Experimental setup for continuously measuring microbial growth with isothermal microcalorimetry. A microcalorimetry instrument equipped with 48 measuring channels is used to measure and record the heat flow. b) Heat flow curves generated from *E. coli* cells at initial concentrations of 10°, 10^{1}, 10^{3}, and 10^{5} CFU/mL.

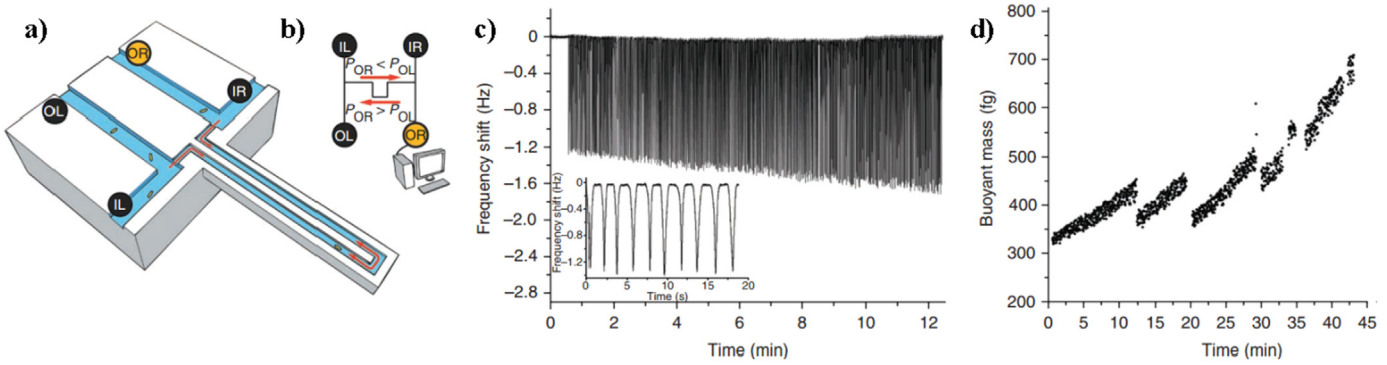

Fig. 20. a) Illustration of the suspended microchannel resonator (SMR) trapping a single cell. Embedded channel cross-sections for microbial cells are 3 × 8 μm. b) Schematic of fluidics: sample is injected in parallel through the left and right inlets (IL and IR) and collected at the left and right outlets (OL and OR). While trapping, IL, IR and OL are kept at a constant pressure. Variable pressure at OR is applied by a computer-controlled regulator that determines the direction of fluid flow in the device. c) Raw data showing 400 measurements of the buoyant mass from one *B. subtilis* cell. The increased frequency shift with time indicates cellular growth. Inset: zoomed detail of a few peaks that show a locally stable baseline that forms after each pass through the SMR, allowing for drift compensation. d) Several *B. subtilis* cells were sequentially trapped. Each point represents the amplitude of the frequency shift, converted to buoyant mass, as the cell transits through the cantilever. Each set of points (for example, from 0 to 12 min) represents one single cell.

numbers with qPCR. The observed exponential increases in 16 S rRNA gene numbers that were directly measured by qPCR were highly reproducible, and thus considered accurate for the estimation of microbial growth. Lankiewicz et al. (2016) reported the application of qPCR assays for analyzing target genes of four marine microbes in pure cultures and in the Delaware estuary environment. One of the limitations of PCR assays is the inability to discriminate between active and inactive cells (Zhang et al., 2017).

8. Comparative features in summary

Every method for the online monitoring of microbial growth is unique invention and capable of addressing special problems under certain conditions. Herein, the general features of the two mainstreams (optics-based methods and electrochemistry-based methods), as well as some of other emerging ones, were summarized for comparison in specificity, sensitivity, instruments involved, simplicity, temporal resolution, accuracy, efficiency and cost (Table 3).

9. Forthcoming trends in online microbial growth monitoring

Though every method discussed above has limitations, some have great potential to advance the development of online and automated methods for monitoring microbial growth. There are significant advantages in optic-based methods. In particular, improvements in mathematical modeling (Tonner et al., 2017), miniaturization of setups (Maia et al., 2016), and the feasibility of more accurate measurements and point-of-care applications results in promising applications of these methods. In addition, advances in imaging methods, and especially lensless methods, will result in greater insight into single cell activities (Jung and Lee, 2016). Thus, it appears that optical methods will remain the primary techniques for online monitoring of microbial growth over the next decade. However, several issues with optic-based methods are worthy of further study, including the requirement of transparency, measurement noise, adhesion of materials, light dispersion by cell debris, and interference from gas bubbles or other micro- and nanoparticles (Qiu et al., 2017). Further, time and cost efficacy, as well as the potential inhibition of fluorescent reagents (Wang et al., 2011), should be considered when developing new optic-based methods.

All of the electrochemistry-based online methods have involved indirect measurements, and do not provide high-resolution measurements (Ahmed et al., 2014; Settu et al., 2015; Yao et al., 2011). To address this problem, electrode deterioration and nonspecific binding are key obstacles should be overcome. Working electrodes coated with Nafion film (Chinnathambi and Euverink, 2018) may represent a significant breakthrough if the auxiliary material does not exhibit any negative effects on biological activities. Furthermore, antifouling electrodes may be an attractive alternative (Hui et al., 2017; Jiang et al., 2016). Moreover, C^4D is another credible candidate for developing methods for online monitoring of microbial growth.

Gene analysis-based methods have great potential in simultaneously measuring growths of multiple target microbes due to their good specificity. However, at present, PCR-based approaches are limited mainly by labor-intensive operations and time consumption (Safavieh et al., 2017). The application of loop-mediated isothermal amplification (LAMP), which exhibits higher efficiency, higher specificity, higher sensitivity and lower cost than PCR (Zhang et al., 2014; Zhao et al., 2015), is promising to overcome these issues. Moreover, the sensitivity of LAMP is less affected by substances that usually inhibit PCR reactions, such as food ingredients and blood components (Abdul-Ghani et al., 2012; Kaneko et al., 2007; Zhang et al., 2014). This is encouraging news for developing online monitoring methods due to the likelihood of eliminating the toughest requirements of sample pretreatments. In addition, high-throughput sequencing (or next-generation sequencing) is also a promising method, provided that we can reduce the cost.

Table 3
Summary features of online methods for monitoring microbial growth.

Category	Summary description	Advantages	Disadvantages	Reference
Optics (non-imaging)	Principle of absorption, diffraction, refraction and scattering, monitoring microbial growth by measuring changes of optical parameters of the cells or medium using photometers	Non-invasive and full automatic manner, free of contamination; capable of managing high workload; high temporal resolution, good accuracy and low cost	Bulky and sophisticated instruments; low specificity and sensitivity	(Maugeri et al., 2018)
Optics (imaging individual cell)	Employing fluorescence or not, directly monitoring morphological, physiological, metabolic or structural characteristics of individual microbes with cameras coupled microscopy	High specificity, sensitivity and temporal resolution	Bulky and sophisticated instruments; accuracy and efficiency depend on the skill of the operator	(Chen et al., 2017; Syal et al., 2017)
Optics (imaging population)	Monitoring population of microbial cells in liquid with lower resolution imaging	Without the need to attach cells to an inert surface; capable of managing high workload; high sensitivity and temporal resolution	Special instrument and imaging algorithms; moderate specificity and accuracy	(Fredborg et al., 2013; Syal et al., 2017)
Optics (visualization)	Utilizing chromogenic or fluorescent probes to show visual changes resulting from microbial growth	High simplicity and low cost	Only suitable for crude assessments; subjective error	(Thakur et al., 2015; Wang et al., 2013)
Electrochemistry(sensor)	Principle of impedance, capacitance, conductivity and voltammetry, monitoring microbial growth by measuring changes of electrochemical parameters of the working electrodes or analytes	Simple, miniaturized and cheap instruments compared to optic-based methods; interference-free from turbidity and color; label free	Low temporal resolution (≥ 5 min), reproducibility, efficiency and sensitivity; nonspecific information	(Ahmed et al., 2014; Maugeri et al., 2018)
Electrochemistry(biosensor)	Monitoring microbial growth by measuring changes of electrochemical parameters resulting from captures of cells or metabolites by biomaterials immobilized on electrodes	Simple, miniaturized and cheap instruments compared to optic-based methods; interference-free from turbidity and color; good specificity	Low temporal resolution (≥ 5 min), reproducibility, efficiency and sensitivity; need of biomaterials and immobilization step	(Ahmed et al., 2014; Syal et al., 2017)
Electrochemistry(contactless sensor)	Monitoring microbial growth by measuring conductivity changes with C^4D or other contactless sensor	The same as electrochemical sensor, plus high reproducibility and temporal resolution; label free	Non-specific response; low sensitivity	(Zhang et al., 2018)
Magnetic bead	Monitoring changes in spin of magnetic beads in a magnetic field as a function of the number of microbe bound	Interference-free from turbidity and color; high sensitivity (individual cell); label free	Bulky and sophisticated instruments; low temporal resolution (≥ 40 min) and efficiency; labor-intensive	(Kinnunen et al., 2011; Sinn et al., 2012)
Microcalorimetry	Measuring cumulative heat and generating heat curves of growing microbial cells	Non-invasive and full automatic manner, free of contamination; high temporal resolution; label free	Bulky and sophisticated instruments; low sensitivity and specificity	(Bonkat et al., 2012)
Resonant mass	Measuring mass changes of individual cell in small channel of cantilever to quantify microbial number	Interference-free from turbidity and color; high sensitivity (individual cell); label free	Sophisticated instruments; only suitable for non-adherent species	(Syal et al., 2017; Godin et al., 2010)
Gene analysis	Monitoring microbial growth by quantifying special genes via amplification with PCR, etc.	Simultaniously achieving identification and quantification, multiple targrt microbial species	Requirements of sampling and other complicated operations (e.g. DNA extraction); low accuracy	(Zhang et al., 2017; Syal et al., 2017)

Electronic tongue/nose can recognize chemical fingerprint patterns through an array of semi-selective sensors for volatile organic compounds with non-invasive manner (Maugeri et al., 2018). Thus they are also promising to be used for simultaneously monitoring microbial growths of different species in the future.

Acknowledgements

This work was supported by the National Key R&D Program of China (2017YFE1015200) and the Special Scientific Research Funds for Central Non-profit Institutes, the Yellow Sea Fisheries Research Institute, Chinese Academy of Fishery Sciences (20603022018020, 20603022016003).

Declarations of interest

none.

References

Abdul-Ghani, R., Al-Mekhlafi, A.M., Karanis, P., 2012. Acta Trop. 122, 233–240.
Ahmed, A., Rushworth, J.V., Hirst, N.A., Millner, P.A., 2014. Clin. Microbiol. Rev. 27, 631–646.
Bonkat, G., Braissant, O., Widmer, A.F., Frei, R., Rieken, M., Wyler, S., Gasser, T.C., Wirz, D., Daniels, A.U., Bachmann, A., 2012. BJU Int. 110, 892–897.
Cermak, N., Olcum, S., Delgado, F.F., Wasserman, S.C., Payer, K.R., Murakami, M.A., Knudsen, S.M., Kimmerling, R.J., Stevens, M.M., Kikuchi, Y., 2016. Nat. Biotechnol. 34, 1052–1059.
Chai, X., Dong, C., Deng, Y., 2008. Anal. Chem. 80, 7820–7825.
Chandra, A., Singh, N., 2018. Chem. Commun. 54, 1643–1646.
Chen, M., Zhao, Z., Yang, J., Peng, K., Baker, M.A., Bai, F., Lo, C.-J., 2017. eLife 6, e22140.
Chinnathambi, S., Euverink, G.J.W., 2018. Sens. Actuators B Chem. 264, 38–44.
Cho, I.-H., Irudayaraj, J., 2013. Int. J. Food Microbiol. 164, 70–75.
Choi, A., Park, J.-S., Jung, H.-I., 2009. Sens. Actuators B Chem. 137, 357–362.
Deris, J.B., Kim, M., Zhang, Z., Okano, H., Hermsen, R., Groisman, A., Hwa, T., 2013. Science 342, 1237435.
Drummond, T.G., Hill, M.G., Barton, J.K., 2003. Nat. Biotechnol. 21, 1192–1199.
Duuren, J.B., Müsken, M., Karge, B., Tomasch, J., Wittmann, C., Häussler, S., Brönstrup, M., 2017. Sci. Rep. 7, 5223.
Ferrer, M., Rodriguez, J., Álvarez, L., Artacho, A., Royo, G., Mira, A., 2017. J. Appl. Microbiol. 122, 640–650.
Fredborg, M., Andersen, K.R., Jørgensen, E., Droce, A., Olesen, T., Jensen, B.B., Rosenvinge, F.S., Sondergaard, T.E., 2013. J. Clin. Microbiol. 51, 2047–2053.
Ghafar-Zadeh, E., Sawan, M., Chodavarapu, V.P., Hosseini-Nia, T., 2010. IEEE Trans. Biomed. Circuits 4, 232–238.
Godin, M., Delgado, F.F., Son, S., Grover, W.H., Bryan, A.K., Tzur, A., Jorgensen, P., Payer, K., Grossman, A.D., Kirschner, M.W., 2010. Nat. Methods 7, 387–390.
Goh, M.C., Borisenko, V., 2017. Anal. Methods 9, 2392–2396.
Gopinath, S.C., Tang, T.-H., Chen, Y., Citartan, M., Lakshmipriya, T., 2014. Biosens. Bioelectron. 60, 332–342.
Hayden, R.T., Clinton, L.K., Hewitt, C., Koyamatsu, T., Sun, Y., Jamison, G., Perkins, R., Tang, L., Pounds, S., Bankowski, M.J., 2016. J. Clin. Microbiol. 54, 2701–2706.
He, B., Liao, L., Xiao, X., Gao, S., Wu, Y., 2009. Biosens. Bioelectron. 24, 1990–1994.
Hodges, H.L., Brown, R.A., Crooks, J.A., Weibel, D.B., Kiessling, L.L., 2018. Proc. Natl. Acad. Sci. 115, 5271–5276.
Huang, S., Pang, P., Xiao, X., He, L., Cai, Q., Grimes, C.A., 2008. Sens. Actuators B Chem. 131, 489–495.
Huang, S., Wang, Y., Ge, S., Cai, Q., Grimes, C.A., 2010. Sens. Actuators B Chem. 150, 412–416.
Hui, N., Sun, X., Niu, S., Luo, X., 2017. ACS Appl. Mater. Interfaces 9, 2914–2923.
Ibarlucea, B., Rim, T., Baek, C., De Visser, J., Baraban, L., Cuniberti, G., 2017. Lab Chip 17, 4283–4293.
Jain, S., Chattopadhyay, S., Jackeray, R., Abid, C.Z., Kohli, G.S., Singh, H., 2012. Biosens. Bioelectron. 31, 37–43.
Jakiela, S., Kaminski, T.S., Cybulski, O., Weibel, D.B., Garstecki, P., 2013. Angew. Chem. Int. Ed. 52, 8908–8911.
Jiang, C., Alam, M.T., Parker, S.G., Darwish, N., Gooding, J.J., 2016. Langmuir 32, 2509–2517.
Jo, N., Kim, B., Lee, S.-M., Oh, J., Park, I.H., Lim, K.J., Shin, J.-S., Yoo, K.-H., 2018. Biosens. Bioelectron. 102, 164–170.
Jung, J.H., Lee, J.E., 2016. Sci. Rep. 6, 21473.
Jung, M.Y., Lee, J., Park, B., Hwang, H., Sohn, S.-O., Lee, S.H., Lim, H.I., Park, H.W., Lee, J.-H., 2017. Food Microbiol. 64, 33–38.
Kaneko, H., Kawana, T., Fukushima, E., Suzutani, T., 2007. J. Biochem. Biophys. Methods 70, 499–501.
Kim, Y.-H., Park, J.-S., Jung, H.-I., 2009. Sens. Actuators B Chem. 138, 270–277.
Kinnunen, P., Sinn, I., McNaughton, B.H., Newton, D.W., Burns, M.A., Kopelman, R., 2011. Biosens. Bioelectron. 26, 2751–2755.
Knudsen, S.M., von Muhlen, M.G., Schauer, D.B., Manalis, S.R., 2009. Anal. Chem. 81, 7087–7090.
Koch, A.L., 2007. Growth Measurement. Category: Microbial Genetics and Molecular Biology. American Society of Microbiology, pp. 172–197.
Kocincová, A.S., Nagl, S., Arain, S., Krause, C., Borisov, S.M., Arnold, M., Wolfbeis, O.S., 2008. Biotechnol. Bioeng. 100, 430–438.
Kuru, E., Tekkam, S., Hall, E., Brun, Y.V., Van Nieuwenhze, M.S., 2015. Nat. Protoc. 10, 33.
Kuswandi, B., Larasati, T.S., Abdullah, A., Heng, L.Y., 2012. Food Anal. Methods 5, 881–889.
Lankiewicz, T.S., Cottrell, M.T., Kirchman, D.L., 2016. ISME J. 10, 823.
Lee, C.-S., Kim, S.K., Kim, M., 2009. Sensors 9, 7111–7131.
Leonard, H., Halachmi, S., Ben-Dov, N., Nativ, O., Segal, E., 2017. ACS Nano 11, 6167–6177.
Lin, H.L., Lin, C.C., Lin, Y.J., Lin, H.C., Shih, C.M., Chen, C.R., Huang, R.N., Kuo, T.C., 2010. Appl. Environ. Microbiol. 76, 1683–1685.
London, R., Schwedock, J., Sage, A., Valley, H., Meadows, J., Waddington, M., Straus, D., 2010. PloS One 5, e8609.
Maia, M.R., Marques, S., Cabrita, A.R., Wallace, R.J., Thompson, G., Fonseca, A.J., Oliveira, H.M., 2016. Front. Microbiol. 7, 1381.
Mao, J., Yan, Y., Olaf, E., Chen, X., Wang, Z., Cui, J., 2017. Bioprocess. Biosyst. Eng. 22, 161–169.
Matsuura, K., Asano, Y., Yamada, A., Naruse, K., 2013. Sensors 13, 2484–2493.
Maugeri, G., Lychko, I., Sobral, R., Roque, A.C.A., 2018. Biotechnol. J. 1700750.
McBirney, S.E., Trinh, K., Wong-Beringer, A., Armani, A.M., 2017. Using wavelength-normalized optical spectroscopy to improve the accuracy of bacteria growth rate quantification. Imaging, Manipulation, and Analysis of Biomolecules, Cells, and Tissues XV, p. 1006817. International Society for Optics and Photonics.
Ong, K., Wang, J., Singh, R., Bachas, L., Grimes, C., 2001. Biosens. Bioelectron. 16, 305–312.
Peris, M., Escuder-Gilabert, L., 2013. Anal. Chim. Acta 804, 29–36.
Qiu, T.A., Nguyen, T.H.T., Hudson-Smith, N.V., Clement, P.L., Forester, D.-C., Frew, H., Hang, M.N., Murphy, C.J., Hamers, R.J., Feng, Z.V., 2017. Anal. Chem. 89, 2057–2064.
Safavieh, M., Pandya, H.J., Venkataraman, M., Thirumalaraju, P., Kanakasabapathy, M.K., Singh, A., Prabhakar, D., Chug, M.K., Shafiee, H., 2017. ACS Appl. Mater. Interfaces 9, 12832–12840.
Schuler, M.M., Marison, I.W., 2012. Appl. Microbiol. Biotechnol. 94, 1469–1482.
Settu, K., Chen, C.-J., Liu, J.-T., Chen, C.-L., Tsai, J.-Z., 2015. Biosens. Bioelectron. 66, 244–250.
Shao, J., Xiang, J., Axner, O., Ying, C., 2016. Appl. Opt. 55, 2339–2345.
Si, Y., Grazon, C., Clavier, G., Rieger, J., Audibert, J.-F., Sclavi, B., Méallet-Renault, R., 2016. Biosens. Bioelectron. 75, 320–327.
Sinn, I., Albertson, T., Kinnunen, P., Breslauer, D.N., McNaughton, B.H., Burns, M.A., Kopelman, R., 2012. Anal. Chem. 84, 5250–5256.
Sun, P., Liu, Y., Sha, J., Zhang, Z., Tu, Q., Chen, P., Wang, J., 2011. Biosens. Bioelectron. 26, 1993–1999.
Syal, K., Mo, M., Yu, H., Iriya, R., Jing, W., Guodong, S., Wang, S., Grys, T.E., Haydel, S.E., Tao, N., 2017. Theranostics 7, 1795.
Thakur, B., Amarnath, C.A., Mangoli, S., Sawant, S.N., 2015. Sens. Actuators B Chem. 207, 262–268.
Theophel, K., Schacht, V.J., Schlüter, M., Schnell, S., Stingu, C.-S., Schaumann, R., Bunge, M., 2014. Front. Microbiol. 5, 544.
Tonner, P.D., Darnell, C.L., Engelhardt, B.E., Schmid, A.K., 2017. Genome Res. 27, 320–333.
Toprak, E., Veres, A., Michel, J.-B., Chait, R., Hartl, D.L., Kishony, R., 2012. Nat. Genet. 44, 101.
Varshney, M., Li, Y., 2008. Talanta 74, 518–525.
Varshney, M., Li, Y., 2009. Biosens. Bioelectron. 24, 2951–2960.
von Ah, U., Wirz, D., Daniels, A., 2009. BMC Microbiol. 9, 106.
Wang, S., Lawson, R., Ray, P.C., Yu, H., 2011. Toxicol. Ind. Health 27, 547–554.
Wang, Xd, Meier, R.J., Wolfbeis, O.S., 2013. Angew. Chem. 125, 424–427.
Wawerla, M., Stolle, A., Schalch, B., Eisgruber, H., 1999. J. Food Prot. 62, 1488–1496.
Weidemaier, K., Carruthers, E., Curry, A., Kuroda, M., Fallows, E., Thomas, J., Sherman, D., Muldoon, M., 2015. Int. J. Food Microbiol. 198, 19–27.
Wollenberg, R.D., Donau, S.S., Nielsen, T.T., Sørensen, J.L., Giese, H., Wimmer, R., Søndergaard, T.E., 2016. Pestic. Biochem. Physiol. 134, 24–30.
Yang, L., Banada, P.P., Liu, Y.S., Bhunia, A.K., Bashir, R., 2005. Biotechnol. Bioeng. 92, 685–694.
Yang, L., Bashir, R., 2008. Biotechnol. Adv. 26, 135–150.
Yao, L., Lamarche, P., Tawil, N., Khan, R., Aliakbar, A.M., Hassan, M.H., Chodavarapu, V.P., Mandeville, R., 2011. IEEE Trans. Biomed. Circuits 5, 223–230.
Zhang, L., Narita, Y., Gao, L., Ali, M., Oshiki, M., Okabe, S., 2017. Water Res. 116, 296–303.
Zhang, X., Jiang, X., Yang, Q., Wang, X., Zhang, Y., Zhao, J., Qu, K., Zhao, C., 2018. Anal. Chem. 90, 6006–6011.
Zhang, X., Lowe, S.B., Gooding, J.J., 2014. Biosens. Bioelectron. 61, 491–499.
Zhao, Y., Chen, F., Li, Q., Wang, L., Fan, C., 2015. Chem. Rev. 115, 12491–12545.
Zibaii, M.I., Kazemi, A., Latifi, H., Azar, M.K., Hosseini, S.M., Ghezelaiagh, M.H., 2010. J. Photochem. Photobiol. B, Biol. 101, 313–320.